Diamond & Related Materials 143 (2024) 110913

Contents lists available at ScienceDirect

Diamond & Related Materials

journal homepage: www.elsevier.com/locate/diamond

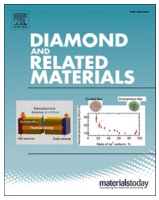

High pressure induced formation of carbon nanorods from tetracosane

Jiaxu Liang [a,1], Christopher P. Ender [a,1], Pascal Rohrbeck [a], Robert Graf [a], Ingo Lieberwirth [a], Hans-Joachim Räder [a], Manfred Wagner [a], Stefan A.L. Weber [a,b], Klaus Müllen [a,c], Tanja Weil [a,*]

[a] Max Planck Institute for Polymer Research, Ackermannweg 10, 55128 Mainz, Germany
[b] Institute of Physics, Johannes Gutenberg University Mainz, Duesbergweg 10-14, 55128 Mainz, Germany
[c] Department of Chemistry, University of Cologne, Greinstr. 4-6, 50939 Cologne, Germany

ARTICLE INFO

Keywords:
Carbon nanorods
High-pressure high-temperature synthesis
Morphology control
Organic pyrolysis
Large volume press

ABSTRACT

Morphology control of carbon structures is essential for improving their performance in many applications. Direct pyrolysis of organic precursors, however, usually yields bulk amorphous carbon. Therefore, traditional methods for controlling the morphology of carbon structures involve multistep processes and complex precursor molecules. While various methods have been developed under ambient pressure, the impact of pressure on the morphology of the resulting carbon structures remains unexplored. Herein, we present the synthesis of carbon nanorods by direct pyrolysis of the low-cost aliphatic hydrocarbon tetracosane under high pressure conditions. The diameters of the carbon nanorods are adjusted by simply varying the synthetic pressures. High pressure allows controlling both the nanorod morphology as well as the degree of order, and local conductivity of the thus prepared nanorods has been confirmed by conductive atomic force microscopy measurements. Our method promises a convenient strategy to synthesize carbon structures with controlled morphology and high ordered chemical structure, which opens opportunities for potential electronic and electrochemical applications.

1. Introduction

Carbon structures have received much attention as functional elements in electrochemical devices, for gas adsorption and storage, as catalysts, and drug delivery systems based on their unique morphologies [1–3]. Specifically, one-dimensional (1D) carbon structures offer unique advantages due to their inherent high-aspect-ratio structural feature. 1D carbon structures can assemble into interconnected networks for flexible electronic materials with improved mechanical elasticity compared to bulk materials or sphere-like nanoparticles [4]. The 1D configuration can also provide continuous ion/electron channels and short diffusion distance for electrolyte ions when they are used in electrochemical devices [5,6]. But convenient synthesis of well-defined 1D carbon structures remains a major challenge because the pyrolysis process for the preparation of carbon materials normally gives amorphous structures. To obtain 1D carbon structures, templates are widely used such as anodic aluminum oxide or mesoporous silica [3]. Alternatively, carbon nanorods have been synthesized by thermal transformation of rod-shaped metal–organic frameworks [7] or electrochemical deposition of a large polycyclic aromatic hydrocarbon (PAH) [8]. These methods, however, involve multistep wet chemistry processes, expensive precursors or hazardous chemicals, and the sizes of the products are difficult to adjust due to the limitation of the templates or precursors. Noteworthy, these traditional methods are in most cases conducted under ambient pressure. However, pressure represents an important parameter that affects chemical bonds, phase transformation and thermodynamic properties of materials [9]. Exploring the synthesis of carbon structures at higher pressures, particular in the gigapascal (GPa) range, could provide access to controlled morphologies.

High-pressure studies of the interactions, reactions, and transformations of atoms or molecules have attracted emerging interest [10,11]. It has been demonstrated that chemical reactions often proceed in an unpredictable fashion and new materials with exciting properties can be formed under high pressure. In the case of carbon materials, high pressure enables phase transition of carbon, along with the transformation from sp^2-hybridized to sp^3-hybridized atoms [12]. Therefore, high-pressure high-temperature (HPHT) techniques are commonly used to synthesize diamonds from all kinds of carbon allotropes [13–15]. However, most studies on carbon materials under high pressure focus on phase transition or atomic valence change, whereas the effect of

* Corresponding author.
E-mail address: weil@mpip-mainz.mpg.de (T. Weil).
[1] denotes equal contribution

https://doi.org/10.1016/j.diamond.2024.110913
Received 27 October 2023; Received in revised form 10 February 2024; Accepted 11 February 2024
Available online 12 February 2024

pressure on morphology control of carbon structures remains largely unexplored.

Herein, we demonstrate the convenient high-pressure synthesis of carbon nanorods by direct pyrolysis of the low-cost aliphatic hydrocarbon tetracosane in a convenient one-pot process (Fig. 1a). To the best of our knowledge, we report the first pressure-induced synthesis of carbon structures with controlled morphologies. We demonstrate that changing the external pressure from 2.6 GPa to 4.0 GPa affords nanorods with tunable diameters, which opens new avenues for synthesizing customized carbon nanomaterials without the need to prepare structurally complex precursor molecules, solvent or catalysts.

2. Experimental

HPHT syntheses of carbon nanorods were carried out in an end-loaded piston cylinder (see supporting information) capable of holding approximate 80 mg and generating a maximum pressure of 4.2 GPa (Fig. 1a and S1). Tetracosane was used as precursor molecule, which is a low-cost and structurally simple, commercial aliphatic hydrocarbon. Pressure was applied up to the set-points of 1.8, 2.6 and 4.0 GPa, respectively. At the set pressure, the sample was heated with a heating rate of 55 °C/min and held at 550 °C for over 18 h. The reactions yielded in black powders, which were washed with dichloromethane to remove the organic residue. The recovered samples were termed as CNR-X, where X denoted the applied pressure.

The investigation of the formation mechanism was carried out at 2.6 GPa. The samples were treated at 550 °C (heating rate of 55 °C/min) for 1 min, 10 min, 1 h and 4 h, respectively and yielded in a colorless, waxy solid (1 min), brown solid (10 min) and black powders (1 h and 4 h). The products were analyzed without further purification.

For the control experiment under low pressure pyrolysis conditions, a copper capsule filled with tetracosane was put in an evacuated (10^{-3} mbar) and sealed glass ampoule. The ampoule was heated to 550 °C for 2 h in an oven. Afterwards, the glass ampoule was opened at the predetermined breaking point and the sample was extracted as a mixture of a yellow liquid and a black solid.

The Raman spectroscopy was conducted using a customized confocal microscope with 532 nm excitation laser (LaserQuantum Tau532) typically operating at 30 mW output power focused onto the sample using a 10× Mitutoyo air objective with long working distance. The high resolution Transmission electron microscopy (TEM) images, Energy dispersive X-ray spectroscopy (EDX) and selected-area electron diffraction (SAED) were obtained with a field-emission transmission electron microscopy (FE-TEM, Tecnai G2 F20 U-TWIN). Powder X-ray diffraction (PXRD) measurements were performed on a Rigaku SmartLab spectrometer using a Cu K-α anode (λ = 1.5406 Å). The powders were placed on a zero reflection Si substrate. Scanning electron microscopy (SEM) of the samples was conducted using a Hitachi SU8000 instrument. Various spots on the whole sample were evaluated using an acceleration voltage of 1.5 kV. Solid State nuclear magnetic resonance (NMR) measurements have been performed on a Bruker Avance III NMR console operating at 500.22 MHz ^{1}H Larmor frequency using a commercial 2.5 mm magic angle spinning (MAS) double resonance probe at ambient temperature and 25 kHz MAS spinning frequency. The conductive atomic force

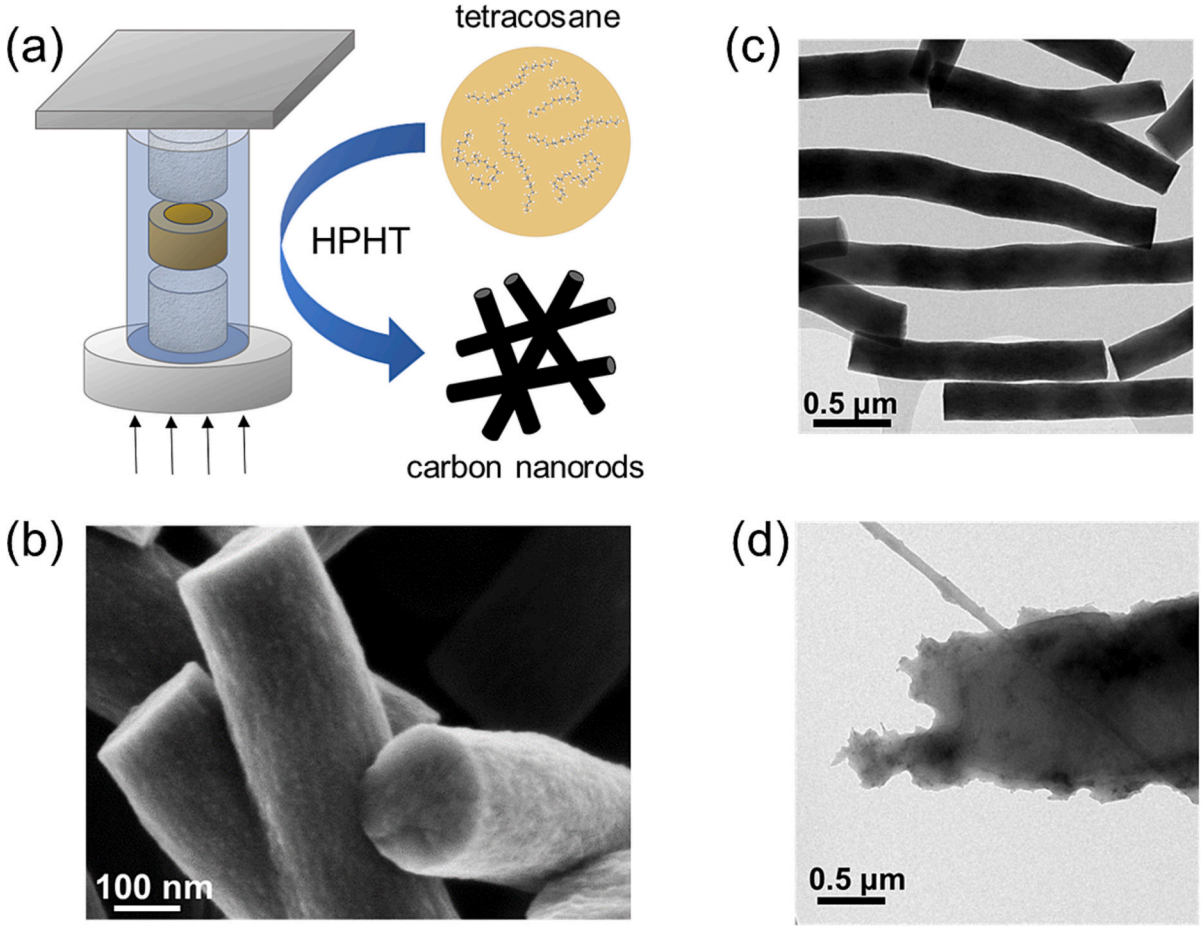

Fig. 1. Synthesis of carbon nanorods from the aliphatic hydrocarbon tetracosane. (a) Illustration of HPHT synthesis of the carbon nanorods with a piston cylinder; (b) SEM image and (c) TEM image of the carbon nanorods synthesized at 550 °C and 2.6 GPa in a piston cylinder; (d) TEM image of the amorphous carbon chunk synthesized at low pressure in a degassed ampoule (10^{-3} mbar).

microscopy (c-AFM) characterizations were performed using an AFM microscope (MFP-3D Infinity, Oxford Instruments Asylum Research Inc.) in nitrogen atmosphere (< 0.1 % humidity, < 0.1 % O_2). c-AFM measurements were carried out with conductive coated (Cr/Au) probes (PNP-TR-Au, Asylum research probes) and an Asylum Research ORCA cantilever holder with a current amplification factor of 50 nA/V.

3. Results and discussion

The SEM analysis of CNR-2.6 revealed the formation of rod-shaped carbon structures with dimensions of around 260 nm wide and typically 1–3 μm in length (Fig. 1b and S2). TEM image further confirmed the formation of carbon nanorods with uniform diameters (Fig. 1c). For comparison, tetracosane was pyrolyzed at 550 °C but at low pressure in a degassed ampoule, and the resulting products consisted of amorphous carbon chunks (denoted as ACC) without any specific shape (Fig. 1d), indicating the crucial role of pressure in the formation of carbon nanorods.

To elucidate the impact of pressure on the dimension of the thus formed carbon nanorods, HPHT experiments were conducted under different pressures. Specifically, the same precursor was heat-treated at 550 °C at 1.8 and 4.0 GPa. We found that the diameters of the carbon nanorods were remarkably affected by the synthesis pressures. The diameters of the recovered carbon nanorods could be adjusted as 652 ± 40 (CNR-1.8), 260 ± 25 (CNR-2.6), 106 ± 20 (CNR-4.0) nm (Fig. 2 and Fig. S3). That is, the diameters of the carbon nanorods reduced with the increase of the synthesis pressures. It was striking that the diameters could be adjusted in a broad range between 100 nm to 600 nm by applying around 2 GPa pressure. These results suggested that pressure could be an efficient tool to manipulate the morphology of carbon nanorods and this straightforward and clean approach could provide an alternative solution for the preparation of defined nanostructures also at larger scales.

Besides morphology, intrinsic chemical structures represent also essential factors to improve the performance of carbon structures in many applications. For example, dangling bonds and defective sites in carbon materials could contribute to their electrochemical reactivity and affect their conductivity when they are used as electrode materials [16,17]. To investigate the impact of pressure on the chemical structures of the formed carbon nanorods, we characterized CNR-2.6 prepared under high pressure and compared it with ACC from low pressure synthesis. EDX in Fig. S4 revealed that carbon was the predominant element in CNR-2.6 with trace amount of oxygen, which could be due to atmospheric oxygen adsorbed on the surface of the nanorods. The chemical structure of CNR-2.6 was further investigated by solid state NMR with $^{1}H—^{13}C$ cross polarization MAS measurement (Fig. 3a). The intense peak at around 122 ppm represented aromatic carbons [18], while the broad asymmetric signal around 22 ppm is assigned to sp^3 carbon moieties. The ratio of sp^2 carbon to sp^3 carbon was estimated to be 95:5, indicating a main product of graphitic carbon. In contrast to the literature using similar aliphatic precursors [19–21], the relatively low pressure in combination with the absence of a diamondoid seed prevents the formation of diamonds. Considering the broad and featureless ^{1}H signal, one could assume the presence of residual methyl groups and methylene in the carbon matrix, originating from the aliphatic precursor. Although a quantitative version [22] of the CP-MAS method has been applied, it should be noted that there might be a systematic tendency to overestimate the content of protonated sp^3 carbon. PXRD revealed the crystalline structures of CNR-2.6 and ACC (Fig. 3b). The characteristic peaks of the graphitic carbon (002) diffraction suggested that both samples were composed of graphitic carbon sheets. However, ACC exhibited a broad peak at 25.0°, whereas CNR-2.6 showed a much sharper peak, indicating larger domain sizes of the graphitic sheets after high-pressure synthesis [23]. Notably, the (002) peak position of CNR-2.6 was centered at 26.0°, larger than that of ACC and similar to that of graphite [23] suggesting that the distances between the graphitic sheets for CNR-2.6 were smaller indicating that high pressure resulted in more closely packed graphitic sheets. CNR-1.8 and CNR-4.0 also revealed similar XRD patterns with sharp peaks at around 26.0° (Fig. S5). The crystalline lattices of CNR-2.6 were also visible under high-resolution TEM (Fig. S6a) and here, the graphitic sheets were stacked along the rod axis. A dominant crystal plane corresponding to d-spacing of 3.6 Å was found by SAED (Fig. S6b), which was close to the interplanar spacing of graphite and confirmed an ordered layer structure [24]. Raman I_D/I_G ratio (where I_D and I_G are D-band and G-band Raman intensities) is another indicator widely used to evaluate the quality of carbon chemical structures [25]. The lower intensity ratio (I_D/I_G) of 1.88 for CNR-2.6 (Fig. 3c), compared to 2.11 for ACC, implied the formation of higher ordered carbon structures under high-pressure synthesis [26], which was in accordance with the XRD and TEM results. The I_D/I_G of CNR-1.8 and CNR-4.0 were 1.90 and 1.76, respectively (Fig. S7), which were similar to that of CNR-2.6. Our results clearly demonstrate that high pressure facilitated the formation of rod-shaped carbon structures with increasing degree of order of the graphitic carbon sheets, leading to higher crystallinity and greater extend of graphitization.

To understand the formation mechanism of carbon nanorods, we collected the products at varying durations of heating under 2.6 GPa. The SEM images (Fig. 4a) reveal the inception of rod-shaped structures after 10 min, albeit with an initially rough surface. Extending the heating time to 1 h remarkably refines the nanorods, making their surfaces much smoother. XRD patterns (Fig. 4b) show the emergence of the (002) peak of graphitic carbon after 10 min, which becomes a sharper signal with prolonged heating durations. This consistent evolution suggests an interdependence between the formation of carbon nanorods and the growth of graphitic carbon sheets. The increase in graphitization with increasing reaction time can also be confirmed by MALDI-TOF (Matrix Assisted Laser Desorption/Ionization Time-of-Flight) mass spectrometry (Fig. S8). A detailed analysis of the low molecular weight fraction reveals a huge number of signals which can all be assigned to pure hydrocarbons with different degrees of hydrogen saturation. Whereas short reaction times result in signals with high H/C ratios, long reaction times lead to a maximum degree of unsaturation. Interestingly

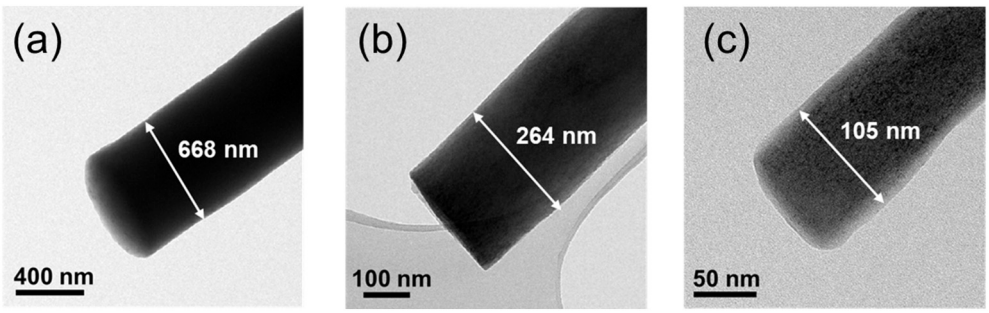

Fig. 2. Carbon nanorods with various diameters synthesized under different pressures. (a) 1.8 GPa; (b) 2.6 GPa; (c) 4.0 GPa.

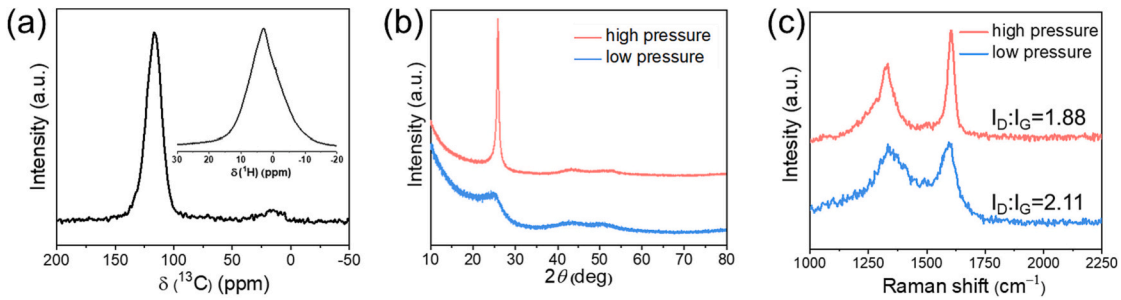

Fig. 3. Structural characterization of the carbon nanorods. (a) Solid state NMR spectra of CNR-2.6 from 550 °C and 2.6 GPa; (b) XRD patterns and (c) Raman spectra of CNR-2.6 (red curves) and ACC (blue curves).

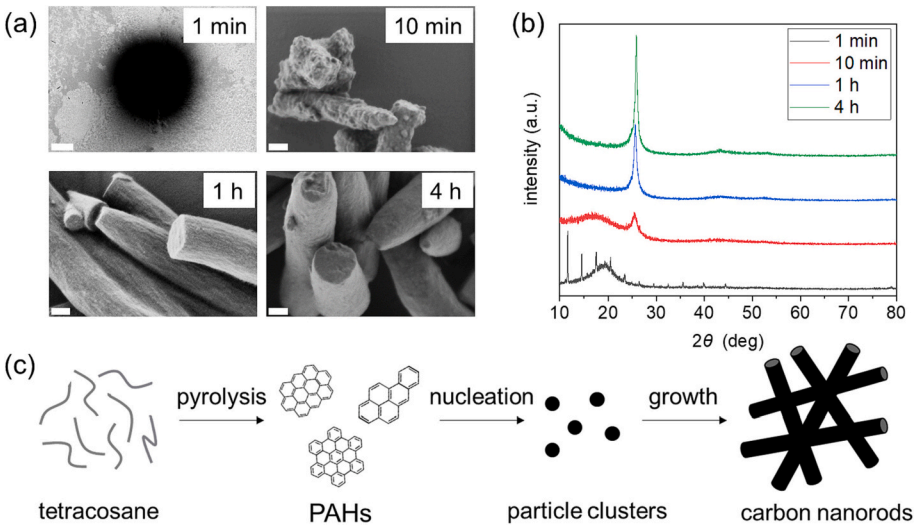

Fig. 4. Growth of the carbon nanorods with heating time. SEM images (a) and XRD patterns (b) of the products after different heating time. The scale bars in (a) represent a length of 100 nm. (c) Proposed formation mechanism of the carbon nanorods.

the measured minimum H/C ratios can all be assigned to two-dimensional polycyclic aromatic hydrocarbons with a maximum degree of unsaturation, thus supporting the assumption for the stacked disc nature of the carbon nanorods.

The proposed mechanism of carbon nanorods formation under pressure is depicted in Fig. 3d. First, tetracosane could decompose into PAHs [27,28]; then these PAHs aggregated to form nucleation clusters of graphitic sheets and grew into the observed rod-shaped nanostructures. Usually, organic precursors form spherical nanoparticles under ambient pressure carbonization which aggregate into commonly observed carbon aerogels. Carbon nanostructures such as nanorods are rarely found because vectorial alignment towards nanorods requires anisotropic Hamaker interaction (force fields) between the graphitic particles [29]. This type of anisotropy could result in preferred orientation of graphitic sheets within the particles. In our case, high pressure could lead to larger sized PAHs as suggested by the above structural characterization, which facilitated the stacking of the graphitic sheets along the rod axis. Furthermore, high pressure could also directly provide an anisotropic force fields, thereby supporting the formation of carbon nanorods.

The high degree of sp^2 hybridization suggested that the carbon nanorods were electrically conductive. To test the electrical properties, we performed c-AFM measurements, where the current between a nanoscale tip and the substrate was measured. Diluted suspensions of CNR-2.6 and CNR-1.8 nanoparticles were deposited on a Si-wafer coated with a thin platinum layer. During imaging, we had to take great care to avoid the sticking of nanorods to the AFM tip (Fig. S9). We therefore selected the fast force mapping mode, where a fast (10–100 Hz) sequence of force-distance curves was performed up to a maximum predetermined load force (2.3 nN in our measurements) and simultaneously recorded the tip-sample current. The height of the individual carbon nanorod of CNR-2.6 was 227 ± 2 nm as shown in Fig. 5(a), which was comparable to the TEM measurements. The current maps clearly showed that the carbon nanorods were electrically conductive with an average vertical current of 680 ± 20 pA measured at a voltage of 10 mV. On the areas surrounding the nanorods, the direct contact between the metallic tip and the Pt substrate led to a saturation of the current amplifier. We also found a similar result on the CNR-1.8 nanorods (Fig. S10). The conductivity value was comparable to carbon black despite that the synthetic temperature of these carbon nanorods was much lower. Furthermore, the structure of nanorods has the advantage to construct conductive percolation network with small amount of material usage [4].

4. Conclusions

In summary, we report a convenient approach to synthesize carbon nanorods based on high pressure chemistry. Since traditional methods for carbon nanostructures are mostly conducted under ambient pressure, we extended the synthesis conditions to higher pressures, for the first time, to investigate the impact of pressure on the morphology control of the resultant carbon nanostructures. Compared to the traditional methods that typically involve multistep reactions and hazardous chemicals, our method used the low-cost aliphatic hydrocarbon tetracosane as precursor in a solvent-free one-pot process. Moreover, the diameters of the carbon nanorods could be adjusted simply by controlling the synthesis pressures. Our results revealed that pressure, as a

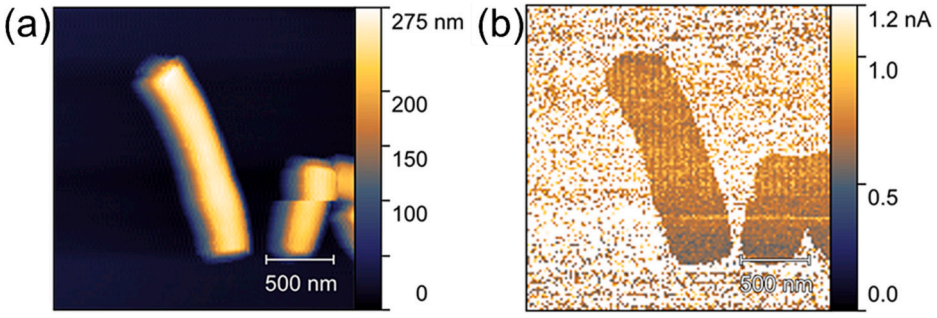

Fig. 5. c-AFM result of CNR-2.6 captured in FFM mode. (a) Topography image of CNR-2.6. The asymmetry in the structure comes from the tip shape (tip convolution effect) (b) Maximum current of each pixel measured at a tip-sample voltage of 10 mV in FFM mode of CNR-2.6. The current signal went into saturation directly on the Pt electrode in the areas around the nanorods.

critical thermodynamic parameter, not only induced the formation of carbon nanorods but also had great impact on the chemical structure of carbon at an atomic level. The local conductivity at the nanoscale was confirmed by conductive AFM, which opens promising applications of these nanorods in electronic and electrochemical devices. We envision that high pressure could be potentially applied for the synthesis of other material systems where morphology control or high-quality crystals are crucial, such as semiconductor nanocrystals, nanostructured metal oxide and various 2D materials for catalysis, optics and magnetic applications.

CRediT authorship contribution statement

Jiaxu Liang: Writing – original draft, Validation, Investigation, Data curation, Conceptualization. **Christopher P. Ender:** Writing – original draft, Validation, Investigation, Data curation, Conceptualization. **Pascal Rohrbeck:** Investigation. **Robert Graf:** Investigation. **Ingo Lieberwirth:** Investigation. **Hans-Joachim Räder:** Investigation. **Manfred Wagner:** Project administration, Conceptualization. **Stefan A.L. Weber:** Writing – review & editing, Methodology. **Klaus Müllen:** Writing – review & editing. **Tanja Weil:** Writing – review & editing, Supervision, Funding acquisition, Conceptualization.

Declaration of competing interest

The authors declare that they have no known competing financial interests or personal relationships that could have appeared to influence the work reported in this paper.

Data availability

Data will be made available on request.

Acknowledgment

The authors are grateful for the financial support from the European Union's Horizon 2020 Research and Innovation Program under FETOPEN grant agreement no. 858149 (AlternativesToGd). The authors thank Gunnar Glaser for SEM measurements, Katrin Kirchhoff for EDX measurements, Jutta Schnee and Stephan Türk for MALDI measurements and Jan Weinheimer for machining the piston cylinder assemblies.

Open access funded by Max Planck Society.

Appendix A. Supplementary data

Supplementary data to this article can be found online at https://doi.org/10.1016/j.diamond.2024.110913.

References

[1] M. Wu, J. Liao, L. Yu, R. Lv, P. Li, W. Sun, R. Tan, X. Duan, L. Zhang, F. Li, J. Kim, K.H. Shin, H. Seok Park, W. Zhang, Z. Guo, H. Wang, Y. Tang, G. Gorgolis, C. Galiotis, J. Ma, Roadmap on carbon materials for energy storage and conversion, Chem-Asian J. 15 (2020) (2020) 995–1013, https://doi.org/10.1002/asia.201901802.

[2] M.R. Benzigar, S.N. Talapaneni, S. Joseph, K. Ramadass, G. Singh, J. Scaranto, U. Ravon, K. Al-Bahily, A. Vinu, Recent advances in functionalized micro and mesoporous carbon materials: synthesis and applications, Chem. Soc. Rev. 47 (2018) 2680–2721, https://doi.org/10.1039/C7CS00787F.

[3] A. Lu, G. Hao, Q. Sun, X. Zhang, W. Li, Chemical synthesis of carbon materials with intriguing nanostructure and morphology, Macromol. Chem. Phys. 213 (2012) 1107–1131, https://doi.org/10.1002/macp.201100606.

[4] S. Gong, W. Cheng, One-dimensional nanomaterials for soft electronics, Adv. Electron. Mater. 3 (2017) 1600314, https://doi.org/10.1002/aelm.201600314.

[5] Q. Wei, F. Xiong, S. Tan, L. Huang, E.H. Lan, B. Dunn, L. Mai, Porous one-dimensional nanomaterials: design, fabrication and applications in electrochemical energy storage, Adv. Mater. 29 (2017) 1602300, https://doi.org/10.1002/adma.201602300.

[6] H. Sun, J. Deng, L. Qiu, X. Fang, H. Peng, Recent progress in solar cells based on one-dimensional nanomaterials, Energy Environ. Sci. 8 (2015) 1139–1159, https://doi.org/10.1039/C4EE03853C.

[7] P. Pachfule, D. Shinde, M. Majumder, Q. Xu, Fabrication of carbon nanorods and graphene nanoribbons from a metal–organic framework, Nat. Chem. 8 (2016) 718–724, https://doi.org/10.1038/nchem.2515.

[8] C. Zeng, W. Zheng, H. Xu, S. Osella, W. Ma, H.I. Wang, Z. Qiu, K. Otake, W. Ren, H. Cheng, K. Müllen, M. Bonn, C. Gu, Y. Ma, Electrochemical deposition of a single-crystalline Nanorod polycyclic aromatic hydrocarbon film with efficient charge and exciton transport, Angew. Chem. Int. Edit. 61 (2022) e202115389, https://doi.org/10.1002/anie.202115389.

[9] P.F. McMillan, Chemistry at high pressure, Chem. Soc. Rev. 35 (2006) 855–857, https://doi.org/10.1039/b610410j.

[10] M. Miao, Y. Sun, E. Zurek, H. Lin, Chemistry under high pressure, Nat. Rev. Chem. 4 (2020) 508–527, https://doi.org/10.1038/s41570-020-0213-0.

[11] L. Zhang, Y. Wang, J. Lv, Y. Ma, Materials discovery at high pressures, Nat. Rev. Mater. 2 (2017) 17005, https://doi.org/10.1038/natrevmats.2017.5.

[12] Y.-P. Xie, X.-J. Zhang, Z.-P. Liu, Graphite to diamond: origin for kinetics selectivity, J. Am. Chem. Soc. 139 (2017) 2545–2548, https://doi.org/10.1021/jacs.6b11193.

[13] J. Dong, Z. Yao, M. Yao, R. Li, K. Hu, L. Zhu, Y. Wang, H. Sun, B. Sundqvist, K. Yang, B. Liu, Decompression-induced diamond formation from graphite sheared under pressure, Phys. Rev. Lett. 124 (2020) 065701, https://doi.org/10.1103/PhysRevLett.124.065701.

[14] M.J. Crane, A. Petrone, R.A. Beck, M.B. Lim, X. Zhou, X. Li, R.M. Stroud, P. J. Pauzauskie, High-pressure, high-temperature molecular doping of nanodiamond, Sci. Adv. 5 (2019) eaau6073, https://doi.org/10.1126/sciadv.aau6073.

[15] C. Pei, L. Wang, Recent progress on high-pressure and high-temperature studies of fullerenes and related materials, Matter Radiat. Extrem. 4 (2019) 028201, https://doi.org/10.1063/1.5086310.

[16] C. Tang, H. Wang, X. Chen, B. Li, T. Hou, B. Zhang, Q. Zhang, M. Titirici, F. Wei, Topological defects in metal-free Nanocarbon for oxygen Electrocatalysis, Adv. Mater. 28 (2016) 6845–6851, https://doi.org/10.1002/adma.201601406.

[17] J. Zhu, Y. Huang, W. Mei, C. Zhao, C. Zhang, J. Zhang, I.S. Amiinu, S. Mu, Effects of intrinsic pentagon defects on electrochemical reactivity of carbon nanomaterials, Angew. Chem. Int. Edit. 58 (2019) 3859–3864, https://doi.org/10.1002/anie.201813805.

[18] Z. Wang, N. Opembe, T. Kobayashi, N.C. Nelson, I.I. Slowing, M. Pruski, Quantitative atomic-scale structure characterization of ordered mesoporous carbon materials by solid state NMR, Carbon 131 (2018) 102–110, https://doi.org/10.1016/j.carbon.2018.01.087.

[19] M. Alkahtani, J. Lang, B. Naydenov, F. Jelezko, P. Hemmer, Growth of high-purity low-strain fluorescent Nanodiamonds, ACS Photonics 6 (2019) 1266–1271, https://doi.org/10.1021/acsphotonics.9b00224.

[20] J. Liang, C.P. Ender, T. Zapata, A. Ermakova, M. Wagner, T. Weil, Germanium iodide mediated synthesis of nanodiamonds from adamantane “seeds” under moderate high-pressure high-temperature conditions, Diam. Relat. Mater. 108 (2020) 108000, https://doi.org/10.1016/j.diamond.2020.108000.
[21] C.P. Ender, J. Liang, J. Friebel, T. Zapata, M. Wagner, A. Ermakova, T. Weil, Mechanistic insights of seeded diamond growth from molecular precursors, Diam. Relat. Mater. 122 (2022) 108796, https://doi.org/10.1016/j.diamond.2021.108796.
[22] R.L. Johnson, K. Schmidt-Rohr, Quantitative solid-state 13C NMR with signal enhancement by multiple cross polarization, J. Magn. Reson. 239 (2014) 44–49, https://doi.org/10.1016/j.jmr.2013.11.009.
[23] T.-H. Kim, E.K. Jeon, Y. Ko, B.Y. Jang, B.-S. Kim, H.-K. Song, Enlarging the d-spacing of graphite and polarizing its surface charge for driving lithium ions fast, J. Mater. Chem. A 2 (2014) 7600–7605, https://doi.org/10.1039/C3TA15360F.
[24] T. Mori, H. Tanaka, A. Dalui, N. Mitoma, K. Suzuki, M. Matsumoto, N. Aggarwal, A. Patnaik, S. Acharya, L.K. Shrestha, H. Sakamoto, K. Itami, K. Ariga, Carbon Nanosheets by morphology-retained carbonization of two-dimensional assembled anisotropic carbon Nanorings, Angew. Chem. Int. Edit. 57 (2018) 9679–9683, https://doi.org/10.1002/anie.201803859.
[25] A. Jorio, A.G. Souza Filho, Raman studies of carbon nanostructures, Annu. Rev. Mater. Res. 46 (2016) 357–382, https://doi.org/10.1146/annurev-matsci-070115-032140.
[26] J. Zhou, J. Lian, L. Hou, J. Zhang, H. Gou, M. Xia, Y. Zhao, T.A. Strobel, L. Tao, F. Gao, Ultrahigh volumetric capacitance and cyclic stability of fluorine and nitrogen co-doped carbon microspheres, Nat. Commun. 6 (2015) 8503, https://doi.org/10.1038/ncomms9503.
[27] J. Ding, L. Zhang, Y. Zhang, K.-L. Han, A reactive molecular dynamics study of n -heptane pyrolysis at high temperature, J. Phys. Chem. A 117 (2013) 3266–3278, https://doi.org/10.1021/jp311498u.
[28] J.W. Martin, L. Pascazio, A. Menon, J. Akroyd, K. Kaiser, F. Schulz, M. Commodo, A. D’Anna, L. Gross, M. Kraft, π-Diradical aromatic soot precursors in flames, J. Am. Chem. Soc. 143 (2021) 12212–12219, https://doi.org/10.1021/jacs.1c05030.
[29] Y. Chang, M. Antonietti, T. Fellinger, Synthesis of nanostructured carbon through Ionothermal carbonization of common organic solvents and solutions, Angew. Chem. Int. Edit. 54 (2015) 5507–5512, https://doi.org/10.1002/anie.201411685.